Extending the plasmonic lifetime of tip-enhanced Raman spectroscopy probes†

Naresh Kumar,*[ab] Steve J. Spencer,[a] Dario Imbraguglio,[c] Andrea M. Rossi,[c] Andrew J. Wain,[a] Bert M. Weckhuysen[b] and Debdulal Roy*[a]

Tip-enhanced Raman spectroscopy (TERS) is an emerging technique for simultaneous mapping of chemical composition and topography of a surface at the nanoscale. However, rapid degradation of TERS probes, especially those coated with silver, is a major bottleneck to the widespread uptake of this technique and severely prohibits the success of many TERS experiments. In this work, we carry out a systematic time-series study of the plasmonic degradation of Ag-coated TERS probes under different environmental conditions and demonstrate that a low oxygen (<1 ppm) and a low moisture (<1 ppm) environment can significantly improve the plasmonic lifetime of TERS probes from a few hours to a few months. Furthermore, using X-ray photoelectron spectroscopy (XPS) measurements on Ag nanoparticles we show that the rapid plasmonic degradation of Ag-coated TERS probes can be correlated to surface oxide formation. Finally, we present practical guidelines for the effective use and storage of TERS probes to improve their plasmonic lifetime based on the results of this study.

1. Introduction

Over the last 15 years, tip-enhanced Raman spectroscopy (TERS)[1] has emerged as an advanced nanoanalytical technique[2] for simultaneous chemical and topographical mapping of surfaces at the nanoscale in diverse areas of scientific research,[3] such as biology,[4] material science,[5] polymer-blends,[6] solar-cells,[7] single-wall carbon nanotubes,[8] graphene and 2D materials,[9–11] catalysis[12–14] and single molecule detection.[15] The principle of TERS is based on the enhancement and confinement of an electromagnetic (EM) field at the apex of a metal or metal-coated scanning probe microscopy tip, when exposed to laser excitation matching its surface plasmon resonance wavelength (λ_{SPR}). This plasmonic enhancement of the EM field underpins the high chemical sensitivity and nanoscale spatial resolution obtained in TERS maps, enabling the observation of molecular phenomena beyond the optical diffraction limit.

Due to plasmonic resonances in the visible light regime, Ag and Au are the most commonly used metals for preparing TERS probes with λ_{SPR} of typical Ag- and Au-coated TERS tips falling in the blue-green and yellow-red regions, respectively.[16] Although Au-coated tips are chemically more stable, there is weak adhesion of Au to the surface of typical Si atomic force microscopy (AFM) tips, resulting in metal delamination during TERS imaging[17] and hence significant losses in plasmonic enhancement.[18] In contrast, solid Ag and Ag-coated TERS tips typically show a much higher EM field enhancement due to the lower imaginary part of the dielectric function compared to Au in the visible light regime, which decreases EM losses arising from optical absorption.[18–20] However, although plasmonically superior, Ag TERS tips are chemically less stable and rapidly lose their plasmonic enhancement.[21,22] Opilik *et al.* have recently shown that solid Ag TERS tips become unusable for TERS measurements after 48 hours.[22] Compared to the solid Ag tips, Ag-coated tips are more commonly used because of both their ease of preparation *via* thermal evaporation from commercial AFM probes that are available in a wide variety of shapes and sizes, as well as ease of use during TERS measurements.[23] However, Ag-coated tips are even more susceptible to plasmonic degradation *via* atmospheric corrosion of the much thinner Ag layer. This represents a major bottleneck to the adoption of the technique prohibiting the success of many TERS experiments which often require careful optimisation of experimental conditions prior to the measurement, including the time-consuming procedure of precisely aligning the TERS tip with the laser spot. In practice, by the time the actual TERS

[a] *National Physical Laboratory, Hampton Road, Teddington, Middlesex TW11 0LW, UK. E-mail: naresh.kumar@npl.co.uk, debdulal.roy@npl.co.uk*

[b] *Faculty of Science, Debye Institute for Nanomaterials Science, Utrecht University, Universiteitsweg 99, Utrecht 3584 CG, The Netherlands*

[c] *Istituto Nazionale di Ricerca Metrologica, Strada delle Cacce 91, 10135 Torino, Italy*

† Electronic supplementary information (ESI) available: Schematic of the optical setup, comparison of the size of Ag nanoparticles (NPs) with Ag grains on the TERS tips, table of binding energy of oxygen bonded to Ag, C and Si, time-series O1s of Ag NPs at 0 and 17 hours, table of time-series XPS results on Ag NP samples with thin and thick SiO₂ substrates, principle of bilayer methodology, experimental details of XPS measurements, calculation of sampling depth of O1s electrons within Ag NPs, chemical reactions of Ag with H₂O under ambient conditions. See DOI: 10.1039/c6cp01641c

13710 | *Phys. Chem. Chem. Phys.,* 2016, **18**, 13710–13716

This journal is © the Owner Societies 2016

imaging commences, the Ag-coated tips may already lose their plasmonic enhancement capability significantly. Furthermore, Ag probes must typically be used on the same day of preparation and cannot be stored for longer periods of time.[24]

In this work, we have addressed three questions: (1) how quickly do Ag-coated tips undergo plasmonic degradation; (2) can this degradation be controlled; (3) what is the mechanism of degradation? Herein, we have carried out a systematic set of time-series measurements of the plasmonic lifetime of Ag-coated TERS probes under different environmental conditions in order to gain insights into their plasmonic degradation. We demonstrate that the preservation of the plasmonic enhancement of TERS tips critically depends upon the oxygen and moisture content of the environment in which the probes are stored. To the best of our knowledge, this is the first systematic study of the impact of different environmental conditions on the plasmonic lifetime of Ag-coated TERS tips. Furthermore, to understand the surface chemistry of Ag nanostructures exposed to the ambient environment we have also performed a time-series investigation of the surface chemical composition of Ag nanoparticles using X-ray photoelectron spectroscopy (XPS). Finally, based on the results of this study, we propose strategies for improving the plasmonic lifetime of TERS probes during their storage and use.

2. Experimental details

2.1. TERS system

A bespoke transmission mode TERS system was used for this work that consisted of an inverted confocal microscope (Nikon, Japan) coupled with an AFM (AIST-NT, The Netherlands) on top. A schematic diagram of the TERS set-up is shown in Fig. 1. A Raman spectrometer (Horiba Scientific, UK) with an electron-multiplying charged coupled device detector (Andor Technology, Ireland) was used to measure the Raman spectra in the 300–3700 cm^{-1} spectral range. A frequency doubled Nd:YAG laser with 532 nm wavelength was radially polarised using a liquid crystal polariser (ARCoptix, Switzerland) and focused onto the sample using a 100×, 1.49 NA oil-immersion objective lens (Nikon, Japan). All measurements were conducted in contact-mode AFM with 100 μW laser power incident at the sample. A detailed schematic diagram of the optical set-up is presented in Supplementary Fig. S1 (ESI†).

2.2. Measurement of plasmonic enhancement

The plasmonic enhancement of the Ag-coated tips was monitored over time by measuring the contrast of "tip-in" (near-field) against "tip-out" (far-field) Raman signals, which is defined in the literature as[23]

$$\text{Contrast} = \frac{I_{\text{Tip-in}}}{I_{\text{Tip-out}}} - 1 \qquad (1)$$

where, $I_{\text{Tip-in}}$ and $I_{\text{Tip-out}}$ are the intensity of a Raman band when the TERS tip is in contact and retracted from the sample, respectively. However, in this work the TERS contrast was measured on a bilayer sample using the methodology reported by Kumar et al.[25] This method provides a more accurate measurement
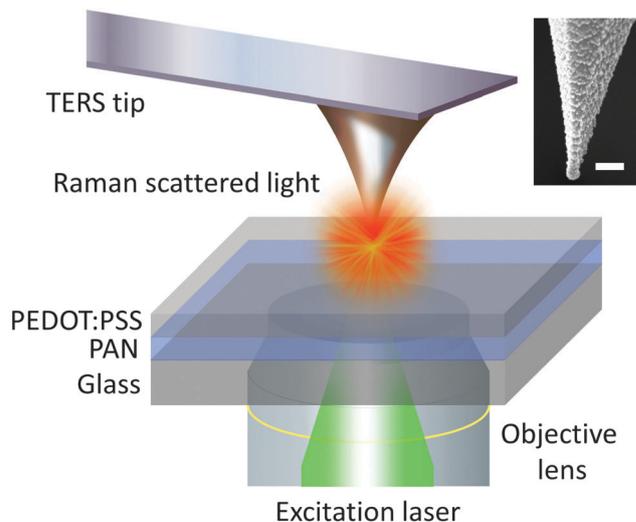

Fig. 1 Schematic diagram of the transmission mode TERS apparatus used in this work. Tip-in (near-field) and tip-out (far-field) measurements were conducted on a bilayer sample (top layer – poly(3,4-ethylenedioxythiophene): poly(styrenesulfonate) (PEDOT:PSS); bottom layer – polyacrylonitrile (PAN)) developed by Kumar et al.[25] A scanning electron microscopy (SEM) image of a representative TERS tip is shown in the inset. Scale bar: 100 nm.

of the contrast of a TERS tip by eliminating the possible far-field artefacts arising from the reflections between the TERS tip and the sample. See Supplementary Note 1 for the principle of bilayer methodology (ESI†).

2.3. TERS tips and time-series measurements

For this study, TERS tips were prepared by first oxidising Si AFM tips (Mikromasch, Estonia) to a thickness of 300 nm SiO_2 in a tube furnace, and then coating them with a nominal thickness of 60 nm Ag. Thermal evaporation of Ag onto the AFM tips was carried out at 10^{-6} mbar pressure with a slow deposition rate of 0.05 nm s^{-1}. An SEM image of a representative TERS tip is shown in the inset of Fig. 1. In this work we investigated the effect of three different environmental conditions on the plasmonic lifetime of TERS tips. First, we studied the effect of ambient conditions on 5 freshly prepared tips that were stored in the laboratory environment immediately after thermal deposition of Ag. For each probe, the contrast of tip-in and tip-out Raman signals was measured at an interval of 4 hours (h) until the probe lost its plasmonic enhancement completely. Secondly, the effect of a vacuum desiccator environment (Duran®, Germany) was tested on 3 sets of 5 TERS tips, with the three different sets measured after storage times of 3, 6 and 9 days. A pressure of 25 mbar was maintained inside the desiccator using an oil-free diaphragm pump (KNF Neuberger Ltd, UK). The plasmonic contrast of the tips was measured at the end of each of these storage times. And finally, the effect of a nitrogen-filled glovebox environment (M. Braun Inertgas-Systeme GmbH, Germany), was tested using 3 sets of 5 TERS tips, this time with the three different sets measured after storage times of 1, 3 and 5 months. Sub-ppm concentrations of oxygen and moisture were maintained in the glovebox by continuous recirculation of nitrogen.

This journal is © the Owner Societies 2016

Phys. Chem. Chem. Phys., 2016, 18, 13710–13716 | 13711

Table 1 Storage conditions of ambient, vacuum desiccator and nitrogen glovebox environments

Environment	Temperature (°C)	Relative humidity (%)	Oxygen (relative to ambient) (%)
Ambient	22.0 ± 0.1	38.7 ± 1.0	100
Vacuum desiccator	22.0 ± 0.1	15.6 ± 1.0	2.5
Nitrogen glovebox	18.8 ± 0.1	0.0 (<1 ppm)	0.0005 (<1 ppm)

The average values of temperature, relative humidity and oxygen in the ambient, vacuum desiccator and nitrogen glovebox environments are listed in Table 1. Relative oxygen concentration is calculated as the % of oxygen concentration relative to the ambient environment (21% of the air). Out of the three environments, nitrogen glovebox contained the lowest moisture and oxygen concentration.

2.4. X-ray photoelectron spectroscopy measurements

To understand the changes in surface chemistry of Ag nanoparticles (NPs) exposed to ambient conditions we carried out time-series XPS measurements on Ag NPs on a Si substrate. This sample was prepared by thermal deposition of a 10 nm thick Ag film on a Si wafer under exactly the same conditions as used for preparing the TERS tips. Topography of the sample was measured using tapping mode AFM. XPS measurements were conducted over time intervals of 0 h (immediately after Ag deposition), 4 h and 17 h in ultra-high vacuum using a Kratos AXIS Ultra DLD (UK) with monochromatic Al Kα excitation. The sample was exposed to the ambient environment in between the measurements similar to the time-series study of TERS tips under ambient conditions. All time-series XPS spectra were acquired from the same location on the Ag NP sample without removing the sample from the sample holder. Further experimental details of the XPS measurements are presented in Supplementary Note 2 (ESI†).

3. Results

3.1. Plasmonic lifetime of TERS tips under different environments

Since most TERS studies are carried out in an ambient environment, we first investigated the plasmonic lifetime of TERS tips under ambient laboratory conditions. Plasmonic enhancement of TERS tips is known to vary from tip to tip.[26,27] Therefore, for a more relevant comparison of the degradation of plasmonic enhancement under different environmental conditions, all time-series TERS measurements were conducted in sets of 5 tips prepared under exactly the same conditions. For the ambient environment, time-series near-field (tip-in) and far-field (tip-out) spectra of 5 freshly prepared TERS tips were measured at intervals of 4 h i.e. at 0, 4 and 8 h. After each TERS measurement, tips were kept in the ambient environment before the next set of measurements. Time-series near-field and far-field spectra of a representative TERS tip are shown in Fig. 2. For the fresh Ag-coated tip (0 h), clear signal enhancement of the characteristic PEDOT Raman peaks (spectral region: 400 cm^{-1} to 1600 cm^{-1})[28]
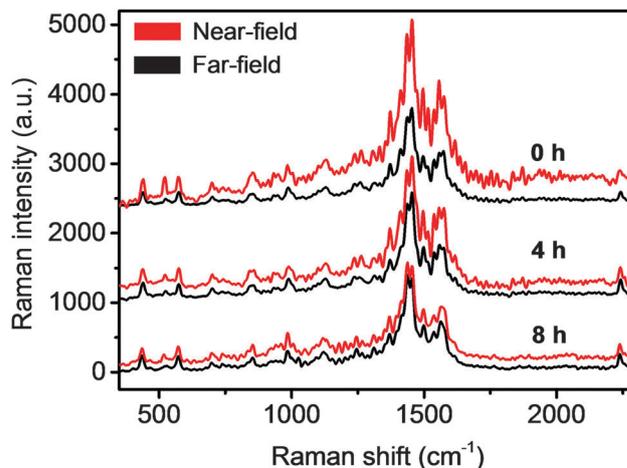

Fig. 2 Time-series near-field and far-field spectra of a representative TERS tip measured at intervals of 4 h under ambient laboratory environment. The plasmonic enhancement rapidly decreases after 4 h and completely disappears after 8 h of exposure to the ambient environment. Laser power at the sample: 100 μW. Integration time: 60 s.

can be observed in the near-field spectrum. The PAN peak at 2247 cm^{-1} is not significantly enhanced in the near-field spectrum, which indicates that there is no significant increase in the undesirable far-field resulting from the reflection between the tip and the sample. The contrast between the near-field and far-field spectra for the fresh Ag-coated tip in Fig. 2 is ≈1. However, after 4 h of exposure to the ambient environment the contrast decreased quite rapidly to ≈0.2 indicating an approximately 80% decrease in the plasmonic enhancement of the tip. Finally, after 8 h of exposure to the ambient environment, the plasmonic enhancement of the TERS tip has essentially vanished with ≈0 contrast between the near-field and far-field spectra. Time-series measurements of the average contrast of 1454 cm^{-1} PEDOT Raman peak from 5 TERS tips are plotted in Fig. 3a that show an exponential decay in the degradation of plasmonic enhancement over time. From this plot the average lifetime of these tips, defined as the time after which their TERS contrast reduces to 1/e times or ≈37% of their initial value, is estimated to be 2.8 h.

Next, we investigated the plasmonic lifetime of TERS tips stored in a vacuum desiccator, which is a commonly used method to preserve TERS tips. Compared to the ambient environment, both relative humidity and oxygen concentration were lower in the vacuum desiccator by 60% and 97.5%, respectively, as listed in Table 1. The average contrast of three different sets of 5 TERS tips measured after storage times of 3, 6 and 9 days, respectively in a vacuum desiccator is shown in Fig. 3b. Comparing Fig. 3a and b, it can be noted that the contrast of freshly prepared tips and the tips stored in the vacuum desiccator for 3 days was similar (≈1) indicating that the vacuum desiccator can successfully preserve the plasmonic enhancement of TERS tips for a few days. However, after 6 days of storage the plasmonic enhancement decreased by 36%. Finally, after 9 days of storage the plasmonic enhancement decreased by 80% and tips were rendered effectively unusable for TERS measurements. The decrease in the oxygen and moisture
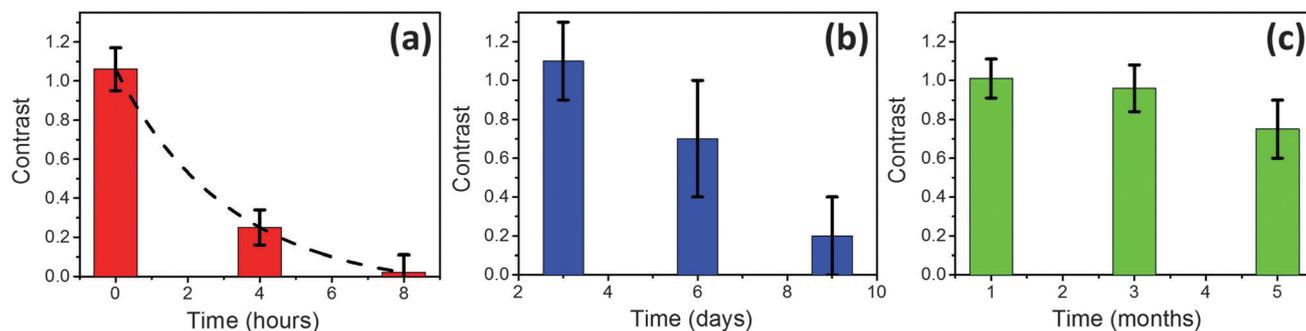
13712 | Phys. Chem. Chem. Phys., 2016, 18, 13710–13716

This journal is © the Owner Societies 2016

Fig. 3 Time-series measurement of plasmonic enhancement *via* TERS contrast of TERS tips stored in (a) ambient (b) vacuum desiccator (c) nitrogen glovebox environments. Under ambient conditions, the plasmonic enhancement decreases rapidly within the first 4 h disappearing completely within 8 h. An exponential decay trend is observed in the plasmonic enhancement within the 8 h period with an average plasmonic lifetime of 2.8 h. The vacuum desiccator environment increases the plasmonic lifetime of TERS tips to a few days. However, the extremely low (<1 ppm) humidity and oxygen concentration inside a nitrogen glovebox provides the best preservation of plasmonic lifetime extending it up to 5 months.

content inside a vacuum desiccator compared to the ambient environment (Table 1) correlates inversely with the average plasmonic lifetime increasing it from a few hours to a few days. Interestingly, the degradation of plasmonic enhancement of TERS tips stored in the vacuum desiccator did not show an exponential trend.

Finally, we investigated the effect of an extremely low moisture and oxygen concentration on the plasmonic lifetime of TERS tips. 3 different sets of 5 TERS tips were stored in a nitrogen glovebox with a moisture concentration of <1 ppm and an oxygen concentration of <1 ppm for periods of 1, 3 or 5 months, before their plasmonic enhancement was measured. Results of these time-series measurements are shown in Fig. 3c. Remarkably, the TERS tips showed a contrast (≈ 1) similar to the freshly prepared tips even after a storage time of 1 month in the nitrogen glovebox, displaying almost no loss of plasmonic enhancement. Furthermore, plasmonic enhancement decreased only marginally by <5% for the tips stored for 3 months. Even after 5 months of storage time the TERS contrast decreased by only <20% indicating that the tips were still usable for TERS measurements. This dramatic increase in the plasmonic lifetime of the TERS tips stored in the nitrogen glovebox underscores the critical role of moisture and oxygen in the rapid degradation of Ag-coated TERS tips. Whilst the TERS tips last for only a few hours in the ambient environment, the extremely low concentration of oxygen and moisture inside a nitrogen glovebox extends their plasmonic lifetime by up to 5 months.

3.2. XPS investigation of silver nanoparticles exposed to ambient environment

To understand the cause of rapid plasmonic degradation of Ag nanostructures under ambient conditions we carried out time-series XPS measurements of Ag NPs on a Si substrate. The Ag NP sample was prepared using similar conditions employed for preparing TERS tips. An AFM topography image of the Ag NPs is shown in Fig. 4a. The typical size of Ag NPs ranges from 11–17 nm. Ag NPs are similar in size to the Ag grains on the surface of Ag-coated tips as shown in Supplementary Fig. S2 (ESI†). For time-series XPS measurements, Ag NPs were exposed

to the ambient laboratory environment for 0 h (immediately after Ag deposition), 4 h and 17 h, respectively.

The O1s spectra of the Ag NPs showed three kinds of oxygen bonding: oxygen bonded to Si (from thermal SiO_2 on the Si wafer), C (from environmental contaminants) and Ag. The binding energies of oxygen in these bonds are listed in Supplementary Table S1 (ESI†). The percentage of oxygen bonded to Si, C and Ag can be determined from the O1s spectra by fitting with three Gaussian–Lorentzian curves as shown in Fig. 4b for the O1s spectrum from Ag NPs measured after 4 h of exposure to the ambient environment. In contrast, the O1s spectrum
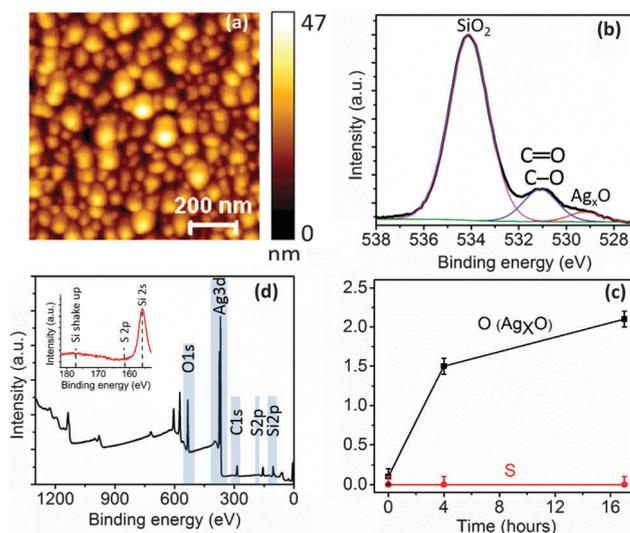

Fig. 4 (a) AFM topography image of Ag NPs on a Si substrate. (b) XPS O1s spectrum of the Ag NPs measured after 4 h of exposure to the ambient environment. Three distinct bands corresponding to the oxygen bonded to Si, C and Ag are fitted with pink, blue and red Gaussian–Lorentzian curves, respectively. (c) Time-series plot of atomic percentage of Ag_xO oxygen and sulphur after 0, 4 and 17 h of exposure to ambient environment. A rapid oxidation of Ag NPs is observed during the first 4 h. (d) XPS survey spectrum and high-resolution S2p spectrum (inset) of Ag NPs measured after 17 h of exposure to the ambient environment. No sulphur was detected on the sample in either spectra.

measured at 0 h showed only a negligible amount (0.1 atomic% of the total elemental composition within the XPS sampling depth) of Ag$_x$O (x = 1 or 2) oxygen as shown in the Supplementary Fig. S4a (ESI†), which rapidly increased to 1.5% after 4 h of exposure to the ambient environment (Fig. 4b). However, subsequently the percentage of Ag$_x$O oxygen on Ag NPs changed only gradually, increasing by only 0.6% in the next 13 h (Supplementary Fig. S4b, ESI†). In the time-series O1s spectra SiO$_2$ peak was observed to shift due to differential charging during XPS measurements. However, the large binding energy difference between SiO$_2$ and Ag$_x$O and careful fitting of the spectra allowed us to reliably calculate the increase in percentage of Ag$_x$O oxygen over time. See Supplementary Fig. S3 for further details of the analysis of O1s spectra (ESI†). The increase in the percentage of Ag$_x$O oxygen over time is plotted in Fig. 4c. The rapid increase in the oxidation of Ag NPs in the first 4 h correlates very well with the rapid decrease in plasmonic enhancement of Ag-coated TERS tips when exposed to the ambient environment. Interestingly, no sulphur could be detected on the Ag NP surface either in the XPS survey spectrum or high resolution S2p spectrum measured after 17 h of exposure to the ambient environment as shown in Fig. 4d. This indicates that for Ag-coated TERS tips, surface oxide formation rather than sulphide tarnishing is the dominant cause of the rapid plasmonic degradation, although sulphide tarnishing of Ag has been observed on solid Ag probes after longer durations of exposure to the ambient environment.[21,22]

Since the binding energies of AgO (528.6 eV) and Ag$_2$O (529.2 eV)[29] are very similar, it is difficult to evaluate the exact contribution of two Ag oxides to the total oxidation on the surface of Ag NPs over time. However, from the XPS measurements it is possible to calculate the atomic percent range of Ag bonded to oxygen at the surface of Ag NPs for each of the different time intervals. It should be noted that 95% of the XPS signal is collected from within an estimated sampling depth of ≈3.3 nm from the surface of Ag NPs (see Supplementary Note 3 for more details, ESI†). The calculation of time-series oxidation of Ag NPs is shown in Table 2. The 2nd column of Table 2 shows Ag$_x$O oxygen as a percentage of total oxygen estimated from the fitted O1s spectra in Supplementary Fig. S4a and b, ESI.† The 3rd column shows Ag$_x$O oxygen as a percentage of total elemental content, estimated by multiplying the total atomic percentage of oxygen in the XPS survey spectra by column 2. The 4th column shows the Ag atomic percentage calculated from the XPS survey spectra. Finally, the 5th column shows the estimated percentage range of Ag atoms oxidised at the Ag NPs surface assuming Ag$_x$O oxygen is distributed uniformly within the XPS sampling depth of ≈3.3 nm. For the freshly prepared Ag NPs,

the percentage of Ag atoms bonded to oxygen at the surface lies between 0.4–0.8%, considering oxidation of all Ag atoms to either AgO or Ag$_2$O, respectively. The actual percentage of oxidised Ag atoms would lie within this range. After 4 h of exposure to the ambient environment the oxidation rapidly rises to 6.4–12.8%, which is quite significant. However, in the next 13 h the % of Ag atoms bonded to oxygen increases rather gradually to 8.8–17.6%. Similar results of Ag$_x$O formation and absence of sulphur were also observed on more Ag NP samples on Si substrates in our laboratory. A summary of these results is presented in Supplementary Table S3 (ESI†). Although similar results of oxide formation and absence of sulphide tarnishing on the surface of Ag nanoparticles exposed to the ambient environment have been reported in the past,[30] the mechanism of oxide formation is rather unclear. However, a clear correlation between corrosion of silver with increasing relative humidity has been observed.[31,32] See Supplementary Note 4 for a description of chemical reactions between Ag and H$_2$O under ambient conditions (ESI†).

3.3. Discussion

Time-series XPS measurements on Ag NPs clearly indicate that a rapid surface oxidation takes place at the Ag surface in the first few hours of exposure to the ambient environment. Since silver oxide is non-plasmonic, it appears to be the dominant cause of the plasmonic degradation of Ag-coated TERS probes. Therefore, the following strategies are proposed to enhance the plasmonic lifetime of Ag-coated TERS tips during storage and use:

• Firstly, any long-term storage (>1 week) or long-distance shipping of Ag-coated probes must be done in a low (ideally with <1 ppm) oxygen and moisture environment, to preserve their plasmonic lifetime effectively. For transporting Ag-coated TERS tips over long distances, specialised sealed containers could be designed that would maintain the oxygen and moisture to <1 ppm level.

• Secondly, TERS measurements should be conducted in an inert (nitrogen or argon) environment with a low oxygen and moisture concentration where possible. This could be achieved either by enclosing the sample and AFM part of the TERS system within a closed box, which can be filled with nitrogen or argon during TERS measurements or by placing the AFM and Raman microscope part of TERS system inside a nitrogen or argon glovebox.

• However, if it is absolutely necessary to perform TERS measurements in ambient environment, Ag-coated TERS tips could be coated with a thin dielectric layer, for example, an ultra-thin (<3 nm) layer of alumina[33] or silica. Although such a coating would slightly decrease plasmonic enhancement,[12] it would block the contact of ambient oxygen and moisture with Ag thereby greatly enhancing the plasmonic lifetime of the tips. However, the dielectric coating must be pinhole-free in order to be effective.

• Finally, if it is not possible to carry out the TERS measurements in an inert environment or protect TERS probes with a thin dielectric coating, then the TERS measurement time especially when using a Ag-coated probe should be kept to a

Table 2 Time-series oxidation of the surface of Ag NPs in ambient environment

Time (hours)	Ag$_x$O oxygen % from O1s spectra	Ag$_x$O oxygen atomic%	Ag atomic%	Estimated % of oxidised Ag atoms
0	0.3	0.1	25.2	0.4–0.8
4	3.6	1.5	23.3	6.4–12.8
17	5.3	2.1	24.0	8.8–17.6

minimum (preferably <1 h). Furthermore, for analysing TERS maps that require more than a few hours of acquisition, the exponential trend of the plasmonic degradation of TERS tip should be taken into account. For such long-acquisition TERS maps, the plasmonic enhancement of the TERS tip could be measured at the beginning and end of the measurement on a reference sample and TERS data could then be normalised in case of significant plasmonic degradation.

4. Conclusions

In this work we have investigated the rapid loss of plasmonic enhancement of Ag-coated TERS probes, which has been a longstanding hurdle in the widespread use of TERS technique so far. We have carried out the first systematic time-series investigation of the plasmonic lifetime of Ag-coated TERS tips under different environmental conditions and shown that the plasmonic enhancement of TERS tips decreases rapidly within the first 4 h of exposure to the ambient environment, disappearing completely within 8 h. Storage in a vacuum desiccator improves the plasmonic lifetime of TERS tips from a few hours to a few days. However, a glovebox environment with sub-ppm oxygen and moisture concentration offers the best preservation of plasmonic enhancement, extending the plasmonic lifetime of the TERS probes up to 5 months. Furthermore, using time-series XPS measurements on Ag NPs we have demonstrated that a rapid oxidation takes place on the surface of Ag NPs within 4 h of exposure to the ambient environment, which correlates negatively with the plasmonic enhancement of TERS tips under similar conditions. Interestingly, no sulphur was detected in any of the XPS spectra indicating that surface oxide formation is the dominant cause of rapid plasmonic degradation of Ag-coated TERS probes. Finally, based on the results of these studies, guidelines for effective use and storage of Ag-coated TERS probes for maximum preservation of their plasmonic lifetime have been proposed. The results of this work are applicable not only to TERS, but also for tip-enhanced fluorescence imaging and surface enhanced Raman spectroscopy, which rely on Ag nanostructures for plasmonic signal enhancement. Therefore, the results presented here are expected to lead to better preservation and transport of Ag-coated probes and improved experimental design, moving TERS and related plasmonic spectroscopies a step closer to becoming routine analytical techniques.

Acknowledgements

Notes and references

1 N. Mauser and A. Hartschuh, *Chem. Soc. Rev.*, 2014, **43**, 1248–1262.
2 C. Blum, L. Opilik, J. M. Atkin, K. Braun, S. B. Kammer, V. Kravtsov, N. Kumar, S. Lemeshko, J. F. Li, K. Luszcz, T. Maleki, A. J. Meixner, S. Minne, M. B. Raschke, B. Ren, J. Rogalski, D. Roy, B. Stephanidis, X. Wang, D. Zhang, J. H. Zhong and R. Zenobi, *J. Raman Spectrosc.*, 2014, **45**, 22–31.
3 N. Kumar, S. Mignuzzi, W. Su and D. Roy, *EPJ Tech. Instrum.*, 2015, **2**, 9.
4 S. Najjar, D. Talaga, L. Schue, Y. Coffinier, S. Szunerits, R. Boukherroub, L. Servant, V. Rodriguez and S. Bonhommeau, *J. Phys. Chem. C*, 2014, **118**, 1174–1181.
5 S. Berweger, C. C. Neacsu, Y. Mao, H. Zhou, S. S. Wong and M. B. Raschke, *Nat. Nanotechnol.*, 2009, **4**, 496–499.
6 L. Xue, W. Li, G. G. Hoffmann, J. G. P. Goossens, J. Loos and G. de With, *Macromolecules*, 2011, **44**, 2852–2858.
7 X. Wang, D. Zhang, K. Braun, H. J. Egelhaaf, C. J. Brabec and A. J. Meixner, *Adv. Funct. Mater.*, 2010, **20**, 492–499.
8 Y. Okuno, Y. Saito, S. Kawata and P. Verma, *Phys. Rev. Lett.*, 2013, **111**, 216101.
9 S. Mignuzzi, N. Kumar, B. Brennan, I. S. Gilmore, D. Richards, A. J. Pollard and D. Roy, *Nanoscale*, 2015, **7**, 19413–19418.
10 A. J. Pollard, N. Kumar, A. Rae, S. Mignuzzi, W. Su and D. Roy, *J. Mater. Nanosci.*, 2014, **1**, 39–49.
11 W. Su, N. Kumar, S. J. Spencer, N. Dai and D. Roy, *Nano Res.*, 2015, **8**, 3878–3886.
12 N. Kumar, B. Stephanidis, R. Zenobi, A. J. Wain and D. Roy, *Nanoscale*, 2015, **7**, 7133–7137.
13 E. M. van Schrojenstein Lantman, T. Deckert-Gaudig, A. J. G. Mank, V. Deckert and B. M. Weckhuysen, *Nat. Nanotechnol.*, 2012, **7**, 583–586.
14 C. E. Harvey and B. M. Weckhuysen, *Catal. Lett.*, 2015, **145**, 40–57.
15 R. Zhang, Y. Zhang, Z. C. Dong, S. Jiang, C. Zhang, L. G. Chen, L. Zhang, Y. Liao, J. Aizpurua, Y. Luo, J. L. Yang and J. G. Hou, *Nature*, 2013, **498**, 82–86.
16 M. Zhang, R. Wang, Z. Zhu, J. Wang and Q. Tian, *J. Opt.*, 2013, **15**, 055006.
17 L. T. Nieman, G. M. Krampert and R. E. Martinez, *Rev. Sci. Instrum.*, 2001, **72**, 1691–1699.
18 T. Schmid, L. Opilik, C. Blum and R. Zenobi, *Angew. Chem., Int. Ed.*, 2013, **52**, 5940–5954.
19 P. B. Johnson and R. W. Christy, *Phys. Rev. B: Solid State*, 1972, **6**, 4370–4379.

This journal is © the Owner Societies 2016

Phys. Chem. Chem. Phys., 2016, **18**, 13710–13716 | **13715**

20 E. Le Ru and P. Etchegoin, *Principles of Surface-Enhanced Raman Spectroscopy: and related plasmonic effects*, Elsevier, 2008.

21 J. Kalbacova, R. D. Rodriguez, V. Desale, M. Schneider, I. Amin, R. Jordan and D. R. Zahn, *Nanospectroscopy*, 2014, **1**, 12–18.

22 L. Opilik, Ü. Dogan, J. Szczerbiński and R. Zenobi, *Appl. Phys. Lett.*, 2015, **107**, 091109.

23 J. Stadler, T. Schmid and R. Zenobi, *Nanoscale*, 2012, **4**, 1856–1870.

24 R. Rodriguez, E. Sheremet, S. Müller, O. Gordan, A. Villabona, S. Schulze, M. Hietschold and D. Zahn, *Rev. Sci. Instrum.*, 2012, **83**, 123708.

25 N. Kumar, A. Rae and D. Roy, *Appl. Phys. Lett.*, 2014, **104**, 123106.

26 A. Hartschuh, E. J. Sanchez, X. S. Xie and L. Novotny, *Phys. Rev. Lett.*, 2003, **90**, 095503.

27 M. S. Anderson and W. T. Pike, *Rev. Sci. Instrum.*, 2002, **73**, 1198–1203.

28 S. Garreau, G. Louarn, J. P. Buisson, G. Froyer and S. Lefrant, *Macromolecules*, 1999, **32**, 6807–6812.

29 J. Moulder, W. Stickle, P. Sobol and K. Bomben, *Handbook of X-ray Photoelectron spectroscopy*, Perkin-Elmer Corporation, USA, 1992.

30 T. Oates, M. Losurdo, S. Noda and K. Hinrichs, *J. Phys. D: Appl. Phys.*, 2013, **46**, 145308.

31 L. Volpe and P. Peterson, *Corros. Sci.*, 1989, **29**, 1179–1196.

32 T. Graedel, *J. Electrochem. Soc.*, 1992, **139**, 1963–1970.

33 C. A. Barrios, A. V. Malkovskiy, A. M. Kisliuk, A. P. Sokolov and M. D. Foster, *J. Phys. Chem. C*, 2009, **113**, 8158–8161.

13716 | *Phys. Chem. Chem. Phys.*, 2016, **18**, 13710–13716

This journal is © the Owner Societies 2016